Interferon lambda 4 expression is suppressed by the host during viral infection

MeeAe Hong,[1]* Johannes Schwerk,[1]* Chrissie Lim,[1]* Alison Kell,[1] Abigail Jarret,[1] Joseph Pangallo,[1] Yueh-Ming Loo,[1] Shuanghu Liu,[2] Curt H. Hagedorn,[3,4] Michael Gale Jr.,[1] and Ram Savan[1]

[1]Department of Immunology, University of Washington, Seattle, WA 98109
[2]Department of Medicinal Chemistry, College of Pharmacy, University of Utah, Salt Lake City, UT 84112
[3]Department of Medicine and [4]Genetics Program, University of Arkansas for Medical Sciences and the Central Arkansas Veterans Healthcare System, Little Rock, AR 72205

Interferon (IFN) lambdas are critical antiviral effectors in hepatic and mucosal infections. Although IFNλ1, IFNλ2, and IFNλ3 act antiviral, genetic association studies have shown that expression of the recently discovered *IFNL4* is detrimental to hepatitis C virus (HCV) infection through a yet unknown mechanism. Intriguingly, human *IFNL4* harbors a genetic variant that introduces a premature stop codon. We performed a molecular and biochemical characterization of IFNλ4 to determine its role and regulation of expression. We found that IFNλ4 exhibits similar antiviral activity to IFNλ3 without negatively affecting antiviral IFN activity or cell survival. We show that humans deploy several mechanisms to limit expression of functional IFNλ4 through noncoding splice variants and nonfunctional protein isoforms. Furthermore, protein-coding *IFNL4* mRNA are not loaded onto polyribosomes and lack a strong polyadenylation signal, resulting in poor translation efficiency. This study provides mechanistic evidence that humans suppress IFNλ4 expression, suggesting that immune function is dependent on other *IFNL* family members.

INTRODUCTION

Type III IFNs are the most recently discovered family of IFNs with antiviral properties. The human *IFN lambda* (*IFNL* or IFNλ) locus is composed of *IFNL1* (*IL29*), *IFNL2* (*IL28A*), *IFNL3* (*IL28B*), and *IFNL4* genes located on chromosome 19 (Kotenko et al., 2003). IFNλs signal through a heterodimeric receptor composed of IFNλR1 and IL-10R2 chains that activate the Jak–STAT pathway to induce IFN-stimulated genes (ISGs) and antiviral activity. Although the antiviral activities of type I and III IFNs are indistinguishable, the type I IFN receptor chains (IFNαR1 and IFNαR2) are nearly ubiquitously expressed, whereas IFNλR1 expression is limited to hepatocytes; epithelial cells of the lung, intestine, and skin; and cells of myeloid lineage (Kotenko et al., 2003; Sheppard et al., 2003; Kotenko, 2011). IFNλ-mediated immunity is essential to fight viral infections in the liver and at epithelial surfaces. *Ifnlr1*$^{-/-}$ mice show that IFNλ activity is required for antiviral protection against respiratory viruses, including the influenza virus and the severe acute respiratory syndrome coronavirus (Mordstein et al., 2008, 2010). In turn, human IFNλ is the dominant IFN secreted by respiratory epithelial cells in response to influenza virus infection (Jewell et al., 2010; Crotta et al., 2013) and is also produced by myeloid and lung epithelial cells during rhinovirus infection (Contoli et al., 2006). Similar to the respiratory tract, epithelial cells of the gastrointestinal tract are predominantly responsive to IFNλ (Mordstein et al., 2010; Pott et al., 2011), which initiates antiviral signaling critical for control of pathogenic enteric viruses (Pott et al., 2011; Mahlakõiv et al., 2015; Nice et al., 2015). Although these studies underscore the importance of IFNλs in antiviral immunity, the expression, regulation, and activities of the individual members of the *IFNL* family during viral infection remain poorly understood.

Genome-wide association studies identified *IFNL* as a strong susceptibility locus for both natural and treatment-induced clearance of HCV (Ge et al., 2009; Suppiah et al., 2009; Tanaka et al., 2009; Thomas et al., 2009; Rauch et al., 2010). Two separate genetic variations in this locus were identified as functionally important for viral clearance (Prokunina-Olsson et al., 2013; McFarland et al., 2014). Our group identified a 3′ untranslated region (UTR) variant in *IFNL3* that dictates the stability and expression of the *IFNL3* mRNA (McFarland et al., 2014) and a subsequent study by Lu et al. (2015b) confirmed these findings. Meanwhile, another study revealed a dinucleotide variant (TT/ΔG, rs368234815) in the *IFNL4* gene that associates with HCV clearance (Prokun-

*M. Hong, J. Schwerk, and C. Lim contributed equally to this paper.

Correspondence to Ram Savan: savanram@uw.edu

Abbreviations used: ActD, actinomycin D; CS, cleavage site; DenV, Dengue virus; EC_{50}, 50% effective concentration; EV, empty vector; HA, hemagglutinin; ISG, IFN-stimulated gene; ISRE, IFN-stimulated response element; PAMP, pathogen-associated molecular pattern; polyA, polyadenylation; poly(I:C), polyinosinic:polycytidylic acid; qPCR, quantitative PCR; RACE, rapid amplification of cDNA ends; rh, recombinant human; RIG-I, retinoic acid–inducible gene I; SeV, Sendai virus; TCA, tricholoroacetic acid; UTR, untranslated region; WNV, West Nile virus.

The Rockefeller University Press $30.00
J. Exp. Med. 2016 Vol. 213 No. 12 2539–2552
https://doi.org/10.1084/jem.20160437

ina-Olsson et al., 2013). A TT variant in the first exon of *IFNL4* creates a premature stop codon, caused by a frameshift, rendering it a pseudogene (*ψIFNL4*; Prokunina-Olsson et al., 2013). Their study showed that a ΔG in *IFNL4* associates with HCV persistence, whereas a TT at the same location correlates with clearance. The study also reports that the ΔG codes for a full-length, functional IFNλ4p179 (179 aa) protein. Surprisingly, HCV persistence is strongly associated with expression of a functional *IFNL4* gene, whereas the nonfunctional *IFNL4* gene is associated with clearance. Although many studies have replicated the strong *IFNL4* association with HCV clearance/persistence, the underlying mechanisms for this paradoxical observation remains unexplained (Aka et al., 2014; Meissner et al., 2014; Lu et al., 2015a,b; O'Brien et al., 2015; Peiffer et al., 2016). Interestingly, the *IFNL4* ΔG allele is in strong linkage with the less favorable *IFNL3* genotype at rs12979860 and rs4803217 (Lu et al., 2015b), suggesting the possibility of an indirect effect of *IFNL4* genotype on HCV persistence. Furthermore, several studies have failed to detect secretion of IFNλ4 protein, prompting speculation on noncanonical activities of IFNλ4, including an intracellular role (Booth and George, 2013; McBride, 2013; Prokunina-Olsson et al., 2013; Ray, 2013; Lu et al., 2015a).

In this study, we use molecular and biochemical approaches to show that IFNλ4 has similar antiviral activities as IFNλ3 but is weakly induced and poorly translated during viral infection. Our investigation revealed that the lower expression of *IFNL4* is due to host adaptation suppressing the functional full-length isoform (179 aa) of *IFNL4* through induction of alternative, nonfunctional, intron-retention splice forms and weak polyadenylation (polyA) signal. This study provides clear mechanistic evidence that humans have sustained adaptations to suppress IFNλ4 expression suggesting that antiviral function is dependent on other *IFNL* family members based on functional and genetic studies.

RESULTS AND DISCUSSION

Bioactivity of IFNλ4 in comparison to IFNλ3

Differential mRNA splicing of the *IFNL4* gene produces three protein-coding isoforms termed *IFNL4P107*, *IFNL4P131*, and *IFNL4P179* based on the number of amino acids encoded (Fig. 1 A). To test their individual activities, we overexpressed IFNλ4p107, IFNλ4p131, and IFNλ4p179 isoforms and IFNλ3, all tagged with C-terminal hemagglutinin (HA) in Huh7 cells. Overexpression was verified by immunoblot using α-HA and α-IFNλ4 antibodies (Fig. 1 B). As the α-IFNλ4 antibody was raised against a peptide encoded in exon 2, this antibody only detects IFNλ4p131 and IFNλ4p179 isoforms. However, α-HA detected equal expression of all IFNλ4 isoforms and IFNλ3 in the whole-cell lysate.

By immunoblotting, we detected two bands in the lysates for IFNλ4p131, IFNλ4p179, and IFNλ3 (Fig. 1 B). These bands usually arise from differential glycosylation, a posttranslational modification that is coded for, and which a majority of IFNs and cytokines require for, efficient secretion and stability. To test if the higher molecular weight bands reflect glycosylated forms of IFNλ4p131, IFNλ4p179, and IFNλ3, we treated the overexpression cell lysates with PNGase F and immunoblotted with α-IFNλ4 and α-HA. We observed that the higher molecular weight band was reduced, indicating that IFNλ4p131 and IFNλ4p179 were glycosylated (Fig. 1 C). Although two bands were detected for IFNλ3, PNGase F failed to reduce the higher molecular weight band, suggesting a non–N-glycosyl modification for IFNλ3.

IFNs require secretion from the cell to engage with their cognate receptors at the cell surface and activate Jak–STAT signaling. To test if the IFNλ4 isoforms were secreted into the supernatant, we performed immunoblots on supernatants, both before (neat) and after concentration by tricholoroacetic acid (TCA) precipitation (Fig. 1 D). When *IFNL* isoforms were overexpressed, we documented secreted IFNλ4p179 and IFNλ3 in both neat and TCA-treated supernatants. However, we did not detect IFNλ4p107 or IFNλ4p131 (Fig. S1 A). These data suggest that IFNλ4p179 and IFNλ3 are released extracellularly, whereas IFNλ4p107 and IFNλ4p131 are retained intracellularly. The supernatants containing IFNλ4p179 or IFNλ3 proteins were then subjected to PNGase F treatment. The higher molecular weight band of IFNλ4p179 was reduced to a lower molecular weight, suggesting that the secreted proteins are also glycosylated (Fig. 1 E).

Another nonsynonymous variant of *IFNL4* (Pro70Ser; rs117648444) exists that changes Proline to Serine at position 70 of the IFNλ4 protein (Prokunina-Olsson et al., 2013; Terczyńska-Dyla et al., 2014). This SNP results in lower activity of IFNλ4, presumably caused by changes in the protein structure, and has been associated with improved spontaneous HCV clearance and better treatment response in patients with ΔG at rs368234815 (Terczyńska-Dyla et al., 2014). We also tested the secretion of IFNλ4p179 S70 (P70S) in comparison to IFNλ4p179 (P70) after expression of both variants in Huh7 cells and found that the S70 variant is secreted less efficiently (Fig. S1 A). Furthermore, expression of *IFNL4P179* S70 (P70S) results in a lower ISG response compared with the *IFNL4P179* P70 variant, as measured by *MX1* quantitative PCR (qPCR; Fig. S1 B). Overall, in our overexpression system, the glycosylated form of IFNλ4p179 is efficiently secreted out of the cell, the P70 variant more than the P70S variant, whereas IFNλ4p107 and IFNλ4p131 are predominantly intracellular.

IFNλ4 signals exclusively through the extracellular IFNλR1–IL-10R2 receptor complex

Similar to other type III IFNs, IFNλ4 is thought to signal through its cognate heterodimeric receptor composed of IFNλR1 and IL-10R2 subunits (Hamming et al., 2013). Type III IFNs evolved from a common lineage with IL-10 family cytokines, many of which feature alternative receptor usage. Because *IFNL4* shares this lineage and has low sequence identity with other type III IFNs (Prokunina-Olsson et al., 2013), we examined if IFNλ4 could also signal through

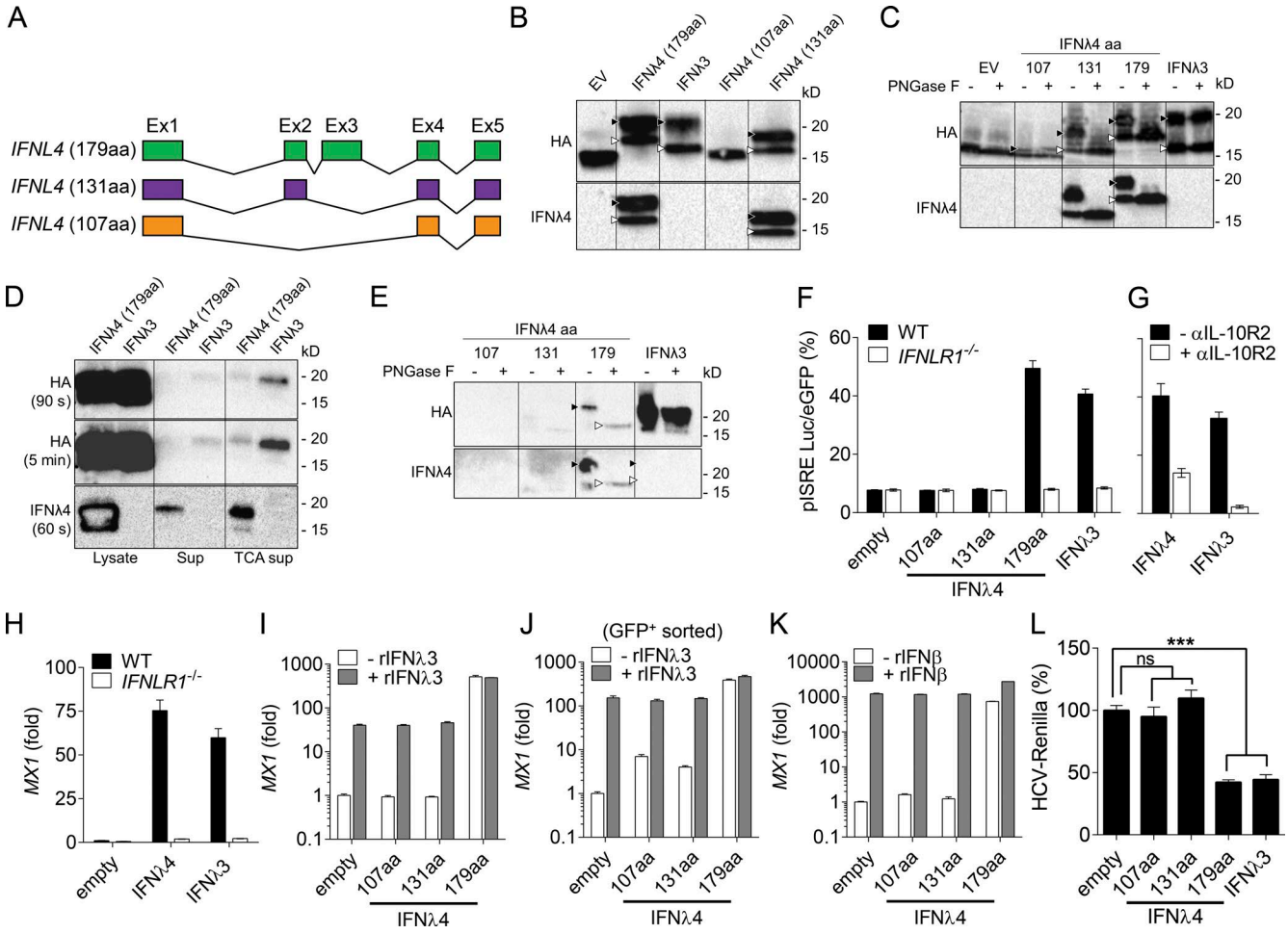

Figure 1. **IFNλ4p179 and IFNλ3 have similar biological activities.** (A) Schematic of the gene structure of protein-coding splice variants of *IFNL4* generated by alternative splicing. (B) Immunoblot of HA-tagged IFNλ3 and IFNλ4 isoforms overexpressed in Huh7 cells. (C) Immunoblot of PNGase F-treated lysates from cells overexpressing HA-IFNλ4 isoforms or HA-IFNλ3. (D) Immunoblot of cell lysates, neat supernatants, and supernatants concentrated by trichloroacetic acid (TCA) treatment. (E) Immunoblot of TCA-treated supernatants of Huh7 cells overexpressing IFNλ4 isoforms. (F) Luciferase reporter assay measuring ISRE activity in wild-type and *IFNLR1*$^{-/-}$ Huh7 cells overexpressing IFNλ3 or IFNλ4 isoforms. (G) Luciferase reporter assay measuring ISRE activity in Huh7 cells treated with IL-10R2–neutralizing antibody and overexpressing IFNλ4p179 and IFNλ3. (H) *MX1* expression in wild-type and *IFNLR1*$^{-/-}$ Huh7 cells overexpressing IFNλ4p179 and IFNλ3. (I–K) *MX1* expression in Huh7 cells overexpressing IFNλ4 isoforms and treated with either IFNλ3 (I and J) or IFNβ (K). (J) *MX1* expression after co-transfection of a GFP plasmid along with the *IFNL4* and *IFNL3* overexpression constructs sorting of GFP^{+} cells directly before IFNλ3 stimulation for 9 h. (L) *Renilla* luciferase reporter activity measured in Huh7 cells overexpressing IFNλ3 or IFNλ4 isoforms infected with HCV tagged with *Renilla* luciferase. Experiments are representative of at least two to three biological replicates. (B–E) Filled arrowheads, glycosylated forms; empty arrowheads, deglycosylated forms. Statistical analysis was performed using one-way ANOVA with multiple comparisons against EV-transfected cells (L). ***, $P < 0.001$; ns, not significant.

a different IL-10 family receptor. We coexpressed the *IFNL4* isoforms and *IFNL3* together with a luciferase reporter downstream of an IFN stimulated response element (ISRE) in Huh7 wild-type and *IFNLR1*$^{-/-}$ cells. We expressed the *IFNL4* isoforms and *IFNL3* in Huh7 cells. Cell supernatants were then transferred to Huh7 wild-type and *IFNLR1*$^{-/-}$ cells expressing a luciferase reporter downstream of an ISRE. We found that expression of IFNλ4p179, the only secreted isoform, and IFNλ3 strongly induced ISRE luciferase reporter activity in wild-type Huh7 cells, whereas the nonsecreted IFNλ4p107 and IFNλ4p131 were inactive (Fig. 1 F). ISRE luciferase reporter activity was completely abrogated in *IFNLR1*$^{-/-}$ Huh7 cells, suggesting that IFNλR1 was necessary for ISG induction by IFNλ4p179. To further test if IFNλ4 signals through extracellular IL-10R2, we blocked the receptor using a neutralizing αIL-10R2 antibody and coexpressed IFNλ4p179 or IFNλ3 together with the ISRE luciferase reporter. IL-10R2 blockade decreased ISRE luciferase reporter activity for both IFNλ4p179 and IFNλ3 (Fig. 1 G and Fig. S1 C). Lastly, downstream signaling via *MX1* induction was completely abrogated in *IFNLR1*$^{-/-}$ cells upon stimulation with IFNλ4p179 (Fig. 1 H). These

data not only confirm that IFNλ4 requires both IFNλR1 and IL-10R2 chains, but also shows that it signals through this extracellular heterodimeric receptor complex.

Intracellular IFNλ4 isoforms do not affect type I and III IFN signaling

As the majority of IFNλ4 remain in the cytoplasm, including both functional and inactive isoforms, it has been proposed that intracellular IFNλ4 regulates cell surface IFNλR1 by binding and sequestering IFNλR1 or IL-10R2 in the cytoplasm (Hamming et al., 2013; Prokunina-Olsson et al., 2013). To quantify the effects of IFNλ4 on receptor surface expression and consequent downstream signaling of other type III IFNs, we treated Huh7 cells overexpressing IFNλ4 isoforms or an empty vector (EV) with recombinant human (rh) IFNλ3 for 6 h, and we quantified ISG induction represented by *MX1*. We found that induction of *MX1* by rhIFNλ3 was unaltered in the presence of overexpressed IFNλ4p107 or IFNλ4p131 compared with EV transfection (Fig. 1 I). Again, IFNλ4p179 alone was able to induce *MX1*, and in this overexpression system it does so at similar levels compared with EV-transfected cells treated with 100 ng/ml rhIFNλ3. To exclude that observed *MX1* expression is due to the nontransfected fraction of cells not expressing *IFNL4* isoforms, we cotransfected a GFP plasmid together with the IFNλ4 overexpression constructs and sorted for GFP^+ cells right before IFNλ3 stimulation for 9 h and qPCR analysis. Again, overexpression of IFNλ4p107 and IFNλ4p131 isoforms did not interfere with the cell's ability to respond to exogenous IFNλ3 (Fig. 1 J). We performed the same stimulation with IFNβ and found that overexpression of intracellular IFNλ4 isoforms does not affect type I IFN signaling (Fig. 1 K). These data show that IFNλ4p179 has a similar ability to induce ISGs as rhIFNλ3 and that IFNλ4 isoforms do not interfere with type I or type III IFN-induced ISG responses intracellularly or extracellularly.

Overexpressed IFNλ4p179 and IFNλ3 have comparable antiviral activity on HCV

The IFNλ4 polymorphism (rs368234815) is presumed to be functional because full-length IFNλ4 protein coding potential encoded by the ΔG genotype correlates with HCV persistence (Prokunina-Olsson et al., 2013). This paradoxical association has led to the hypothesis that IFNλ4 may have noncanonical functions, such as blockade of antiviral activity. To test this hypothesis, we overexpressed IFNλ4 isoforms and IFNλ3 in Huh7 cells and infected them with a *Renilla*-luciferase tagged HCV reporter virus (Liu et al., 2011). We observed that IFNλ4p179 and IFNλ3 mediated similar antiviral activity and comparably suppressed HCV replication, whereas the intracellular IFNλ4p107 and IFNλ4p131 isoforms were unable to block HCV replication (Fig. 1 L). These data suggest that IFNλ4p179 has antiviral activities on HCV comparable to IFNλ3 when overexpressed and, indeed, appears to perform similarly to type III IFNs in the context of antiviral defense.

Antiviral activity of rhIFNλ4

To confirm the observations made with our plasmid-based overexpression system, we purified rhIFNλ4p179 (rhIFNλ4) protein using a *Drosophila* Schneider 2 (S2) cell expression system. We cloned the *IFNL4P179* open reading frame with a C-terminal 6xHistidine tag into a construct under control of a copper (II) ion-inducible metallothionein promoter and transfected the expression plasmid into S2 cells. Upon induction by copper (II) sulfate, rhIFNλ4 was secreted into the supernatant, collected for affinity purification on a nickel column, and further isolated by size exclusion chromatography (Fig. 2, A–C). We compared the activities of rhIFNλ3 and rhIFNλ4 by quantifying *MX1* induction as a functional read out in PH5CH8 hepatocytes. The induction pattern of *MX1* over several logs of IFNλ concentration yielded an EC_{50} of 189.1 pM (3.801 ng/ml) for rhIFNλ3 and an EC_{50} of 577.0 pM (11.01 ng/ml) for rhIFNλ4, leading to an EC_{50} ratio of 3.051 (Fig. 2 D). Intriguingly, the largest differences in activity were seen at lower concentrations of IFNλ. These data suggest that IFNλ3 exhibits activity that is marginally higher than that of IFNλ4, although these differences are minimal compared with differences in activities between IFNλ3 and IFNλ2 (Dellgren et al., 2009). We further tested the specificity for downstream STAT signaling in wild-type or $IFNLR1^{-/-}$ PH5CH8 cells (Fig. S2) stimulated with rhIFNβ, rhIFNλ3, or rhIFNλ4 for 15 min (Fig. 2 E). Treatment with rhIFNβ, rhIFNλ3, or rhIFNλ4 induced phosphorylation of STAT1 (pSTAT1), which was completely abrogated in $IFNLR1^{-/-}$ cells, when stimulated with rhIFNλ3 or rhIFNλ4. To confirm downstream gene expression, we treated wild-type or $IFNLR1^{-/-}$ PH5CH8 cells with rhIFNβ, rhIFNλ3, or rhIFNλ4 for 6 h and quantified the induction of ISGs by qPCR. *MX1*, *OAS1*, and *ISG15* were induced by rhIFNλ4 treatment at comparable levels to rhIFNλ3 treatment. This induction was again abrogated in $IFNLR1^{-/-}$ cells (Fig. 2, F–H). Control treatment with rhIFNβ resulted in stronger activation of pSTAT1 and induction of ISGs, regardless of the $IFNLR1^{-/-}$ status.

Because genetic association data show that individuals carrying the in-frame ΔG variant have increased risk of viral persistence, we examined whether IFNλ4 administration had unique detrimental effects on the host that were independent of virus infection alone, e.g., causing increased cell death. To test if IFNλ4 causes cell death, as another potential mechanism rendering IFNλ4 expression detrimental to the host, PH5CH8 cells were treated with either rhIFNλ4 (100 ng/ml), rhIFNλ3 (100 ng/ml), or actinomycin D (ActD; 10 µg/ml). Cell death and confluence were assessed over 70 h using an IncuCyte imaging system. The cells were treated in the presence of Sytox green, a dye which enters dying cells as they lose membrane integrity. Neither IFNλ3 nor IFNλ4 induced cell death, and cell viability was comparable to mock-treated cells (Fig. 2 I and Video 1). ActD-treated cells served as a positive control for cell death in these assays and *MX1* induction was assessed as a control to show similar IFNλ activi-

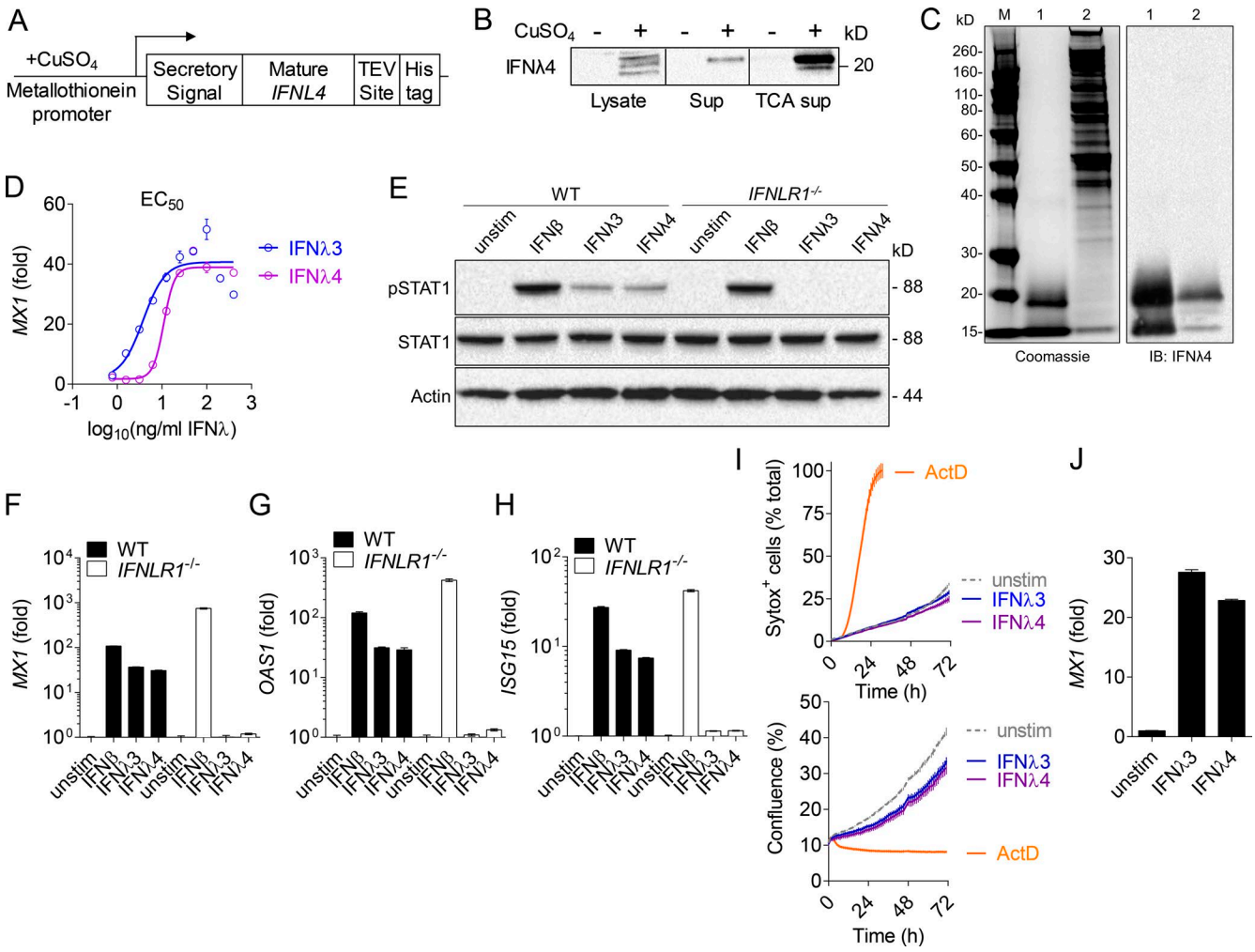

Figure 2. **Recombinant IFNλ4 induces ISGs but not cell death.** (A) Schematic of the plasmid of the inducible expression of rhIFNλ4p179 (rhIFNλ4) in a *Drosophila* S2 Schneider cell expression system. (B) Immunoblot of rhIFNλ4 in lysates, neat supernatants, and supernatants concentrated by TCA treatment upon treatment with or without copper (II) sulfate ($CuSO_4$) for 8 d. (C) Coomassie stain and immunoblot of rhIFNλ4 purified from S2 cell supernatant by affinity chromatography and gel filtration. Lanes: M, molecular weight marker; 1, purified rhIFNλ4; 2, prepurified supernatant. (D) EC_{50} curve of rhIFNλ3 and rhIFNλ4 activity assayed by *MX1* gene expression. (E) Immunoblot of pSTAT1 in wild-type and *IFNLR1*$^{-/-}$ PH5CH8 cells, treated with rhFNβ, rhIFNλ3, and rhIFNλ4. Total STAT1 and β-actin are shown as loading controls; total STAT1 was probed on a separate immunoblot from the same lysates as pSTAT1 and STAT1 antibodies were raised against the same species. (F–H) Gene expression of *MX1* (F), *OAS1* (G), and *ISG15* (H) in wild-type and *IFNLR1*$^{-/-}$ PH5CH8 cells treated with recombinant rhIFNβ, rhIFNλ3, or rhIFNλ4 for 6 h. (I) Proliferation and cell death (object counts) in wild-type PH5CH8 hepatocytes stimulated with rhIFNλ3, rhIFNλ4, and ActD (positive control), measured using Incucyte time-lapse live fluorescent microscopy of a quantifiable cell viability dye, Sytox green, which marks dead cells. (J) *MX1* gene expression measured at 70 h to confirm stimulation of the hepatocytes by rhIFNλ3 and rhIFNλ4 in cell death assays. Experiments are representative of at least two to three biological replicates.

ties (Fig. 2 J). When measured for cell confluence over time as a readout for proliferation, we found that IFNλ3 and IFNλ4 treatment shows a similar antiproliferative effect on cells compared with control cells (Fig. 2 I and Video 1). These data suggest that IFNλ4 does not induce cell death in hepatocytes, which contradicts a previous study that found IFNλ4 could induce cell death (Onabajo et al., 2015). The authors of that study observed differences in the endoplasmic reticulum stress response and cell death in HepG2 cells using a plasmid-based overexpression system; this is in contrast to our use of titrated, recombinant IFNλ proteins, which are likely a cleaner measure of cell death responses that would occur in vivo.

To test if the induction of antiviral ISGs by rhIFNλ4 translates into functional suppression of viral propagation, as we had observed with the use of our plasmid-based overexpression system, we measured replication of HCV (Fig. 3 A) and West Nile virus (WNV; Fig. 3 B) in the presence of rhIFNλ3 or rhIFNλ4. We documented robust antiviral activity against these viruses with rhIFNλ4 treatment, which was comparable to that exerted by rhIFNλ3 (Fig. 3, A and B).

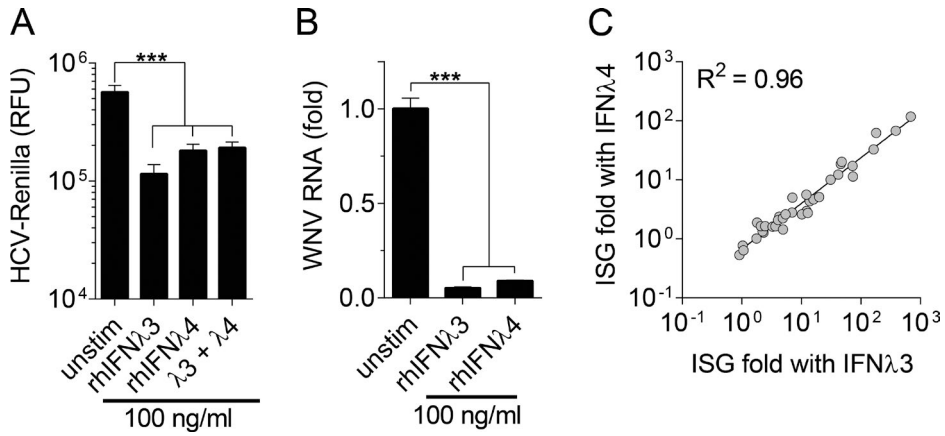

Figure 3. **Recombinant human IFNλ4 shows similar antiviral activity to IFNλ3.** (A) *Renilla* luciferase reporter activity measuring HCV replication in Huh7 cells infected with *Renilla* luciferase-tagged HCV and treated with rhIFNλ3 and rhIFNλ4. (B) WNV RNA load upon treatment of infected Huh7 cells with equal doses of rhIFNλ3 and rhIFNλ4. (C) Correlation of ISG induction in WNV-infected Huh7 cells from B stimulated with 100 ng/ml rhIFNλ3 and rhIFNλ4, based on a TaqMan qPCR array of 37 ISGs. A and B are representative of three independently performed experiments; data in C is from one array. Statistical analysis was performed using one-way ANOVA with multiple comparisons against unstimulated cells (A and B). ***, $P < 0.001$.

Comparable gene induction of 37 ISGs was observed in WNV infection after rhIFNλ3 or rhIFNλ4 treatments (Fig. 3 C and Table 1). These data confirm observations from our overexpression studies and conclusively show that rhIFNλ4 displays antiviral activity comparable to that of IFNλ3.

IFNL4 is expressed at basal levels during viral infection

Previous studies have identified transcripts of the protein-coding isoforms *IFNL4P107*, *IFNL4P131*, and *IFNL4P179* harboring the ΔG allele (Prokunina-Olsson et al., 2013). As the induction pattern of *IFNL4* isoforms during infection is not well documented, we cloned and generated a cDNA library from HepG2 hepatocytes (heterozygotes at rs368234815) stimulated with a retinoic acid–inducible gene I (RIG-I) ligand (HCV 5′ppp RNA) or poly(I:C). Using primers flanking the coding region of *IFNL4P179*, we identified three additional *IFNL4* transcripts with intron retention, which have a similar exon configuration to *IFNL4P107*, *IFNL4P131*, and *IFNL4P179* (Fig. 4, A and B; and Fig. S3). We also identified pseudogenes with premature stop codons carrying the TT allele (Fig. S3). Genes with intron retentions are not exported to the cytoplasm from the nucleus, or are subjected to nonsense-mediated decay in the rare event that export occurs.

To evaluate the induction patterns of these *IFNL4* splice forms by qPCR, we designed primers specific to each protein-coding transcript, as well as a specific primer pair that detects all *IFNL4* isoforms with intron retention (*IFNL4* IR). We established standard curves for these probes and for *IFNL3* to measure absolute copy numbers for each isoform allowing to directly compare abundance across the transcripts (Table 2). Analysis of Huh7 cells (TT/ΔG), HepG2 cells (TT/ΔG), HeLa cells (ΔG/ΔG), and HEK293 cells (ΔG/ΔG) stimulated with the RIG-I ligand HCV 5′ppp RNA (HCV pathogen-associated molecular pattern [PAMP]) and primary human hepatocytes (PHH; TT/ΔG or ΔG/ΔG) stimulated with poly(I:C) revealed that *IFNL3* was highly induced compared with all the *IFNL4* transcripts (Fig. 4, C–F and I–J). Surprisingly, the next most abundant transcripts were *IFNL4* with retained introns, rather than any of the protein-coding isoforms. These were followed by *IFNL4P131*, *IFNL4P179*, and *IFNL4P107* isoforms. As dendritic cells have been reported to express *IFNL1-3* during viral infection (Coccia et al., 2004; Stone et al., 2013), we also stimulated myeloid DC cells differentiated from MUTZ-3 cells (TT/ΔG) and THP-1 cells (TT/ΔG) with poly(I:C) and examined *IFNL* expression patterns (Fig. 4, G and H). Although poly(I:C) induced high *IFNL3* expression in these DCs, the protein-coding *IFNL4* isoforms were not induced, whereas the intron-retaining *IFNL4* transcripts were observed only in THP-1–derived cells that have DC-like characteristics. We found that similar expression patterns, including low-level *IFNL4P179* expression, were seen in hepatoma cells during infections with WNV, Dengue virus (DenV), and Sendai virus (SeV; Fig. 4, K–M). Our data reveal that *IFNL4* is poorly induced compared with *IFNL3* during viral PAMP stimulation and viral infection and that nonfunctional, intron-retaining *IFNL4* isoforms are preferentially transcribed instead of the protein-coding isoforms.

Endogenous *IFNL4* isoforms are not translated efficiently during infection

The poor induction of functional *IFNL4P179* compared with *IFNL3* during viral PAMP stimulation and viral infections would reflect low secretory output of the IFNλ4p179 protein. To test this, we infected Huh7 and HepG2 cells with HCV, WNV, and SeV, and then immunoblotted the cell lysates and supernatants for endogenous IFNλ4 protein. In conformity with previous studies, cell lysates, direct cell cul-

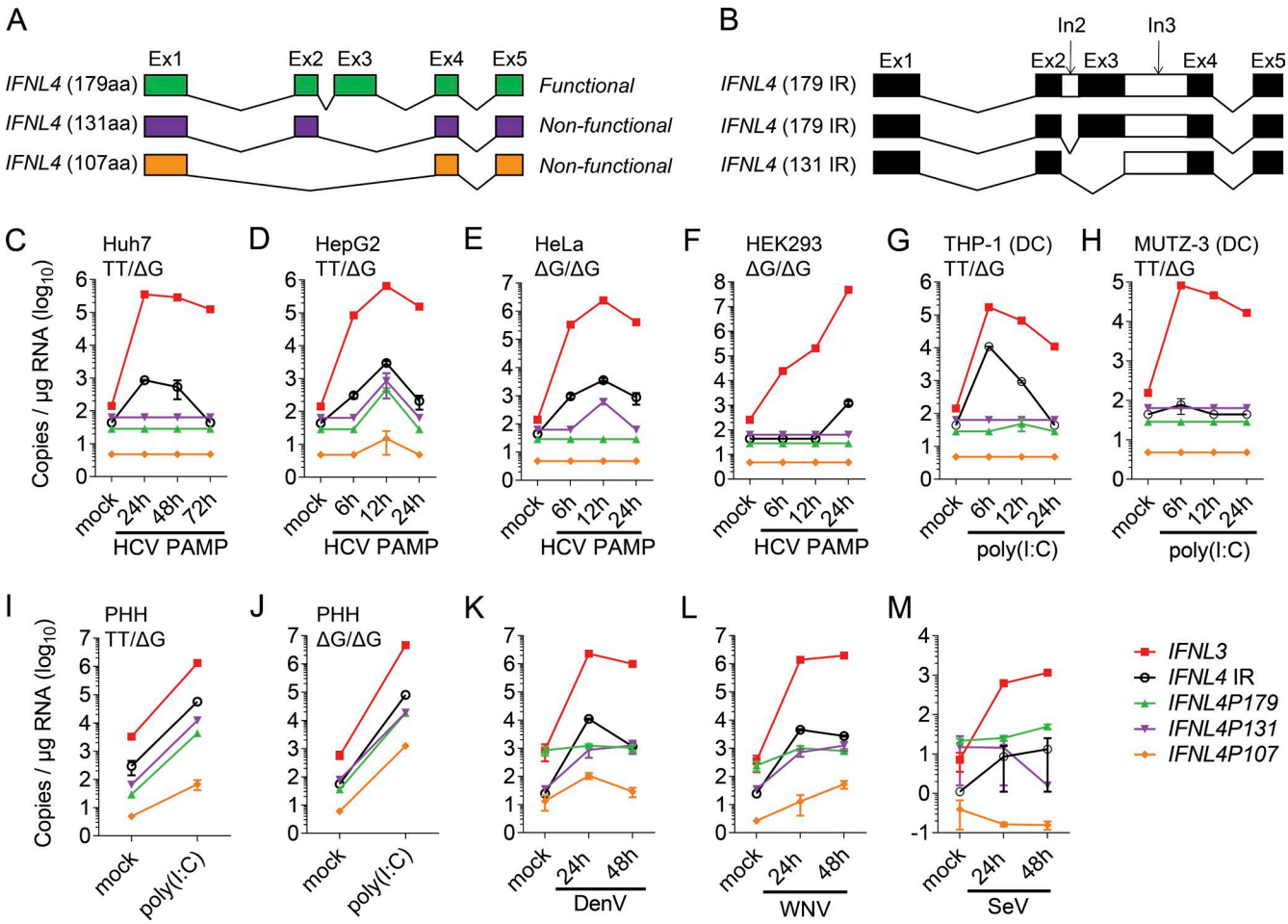

Figure 4. **Low *IFNL4* induction during PAMP stimulation and viral infection.** (A and B) Schematic of *IFNL4* mRNA exhibiting intron retention (IR), compared with the known protein-coding isoforms of *IFNL4*. (C–H) Gene expression kinetics of *IFNL3* and *IFNL4* isoforms measured by qPCR using custom made TaqMan probes in Huh7 (C), HepG2 (D), HeLa (E), and HEK293 (F) cells upon stimulation with HCV PAMP, and DCs derived from THP1 (G) and MUTZ-3 (H) cell lines stimulated with poly(I:C). (I–J) Gene expression of *IFNL3* and *IFNL4* isoforms in primary human hepatocytes, heterozygous (I) or homozygous (J) for the ΔG variant, stimulated with poly(I:C). (K–M) Gene expression of *IFNL3* and *IFNL4* isoforms in HepG2 cells infected with DenV (K), WNV (L), and SeV (M). Experiments are representative of two to three independent experiments (C–H and K–M); experiments on PHHs (I–J) were performed on two biological replicates for each genotype.

ture supernatants, and TCA-concentrated supernatants did not yield detectable IFNλ4 protein. To ensure that this was not a result of poor antibody sensitivity, we performed polysome fractionation to determine efficiency of active translation of *IFNL3* and *IFNL4* isoforms. Cell lysates from HepG2 cells stimulated with poly(I:C) or mock treated for 12 h were separated using a sucrose gradient to separate nontranslating monosome fractions of low centrifugal weight and polysome fractions of high centrifugal weight containing actively translated mRNA (Fig. 5, A–D). Polysome fractions were then pooled and *IFNL3* and *IFNL4* isoforms were quantified by qPCR. Intriguingly, *IFNL4* isoforms were poorly detected (<40 copies) in the heavy polysome and nontranslated monosome fractions, despite detection of high levels of *IFNL3* in these fractions (Fig. 5, C and D), suggesting that *IFNL4* isoforms have only low association with actively translating ribosomal fractions compared with *IFNL3*. Furthermore, the 3′ UTR of *IFNL4*, unlike other *IFNL* genes, does not harbor a canonical polyA signal (Fig. 5 E). For mRNA termination, a polyA signal (canonical motif: AAUAAA) is essential for downstream cleavage and polyA of mRNA. PolyA signal sequences are not only critical for mRNA termination, but also for recruitment of RNA-binding proteins essential for stability and subsequent translation. In silico analysis of the *IFNL4* 3′ UTR did not yield a strong canonical polyA signal compared with the other *IFNL* genes (Fig. S4). To test the polyA signal usage and to identify the downstream cleavage site (CS) essential for *IFNL4* mRNA termination, we used 3′ rapid amplification of cDNA ends (3′ RACE). Cloning and analysis of the 3′ UTRs documented three distinct CSs

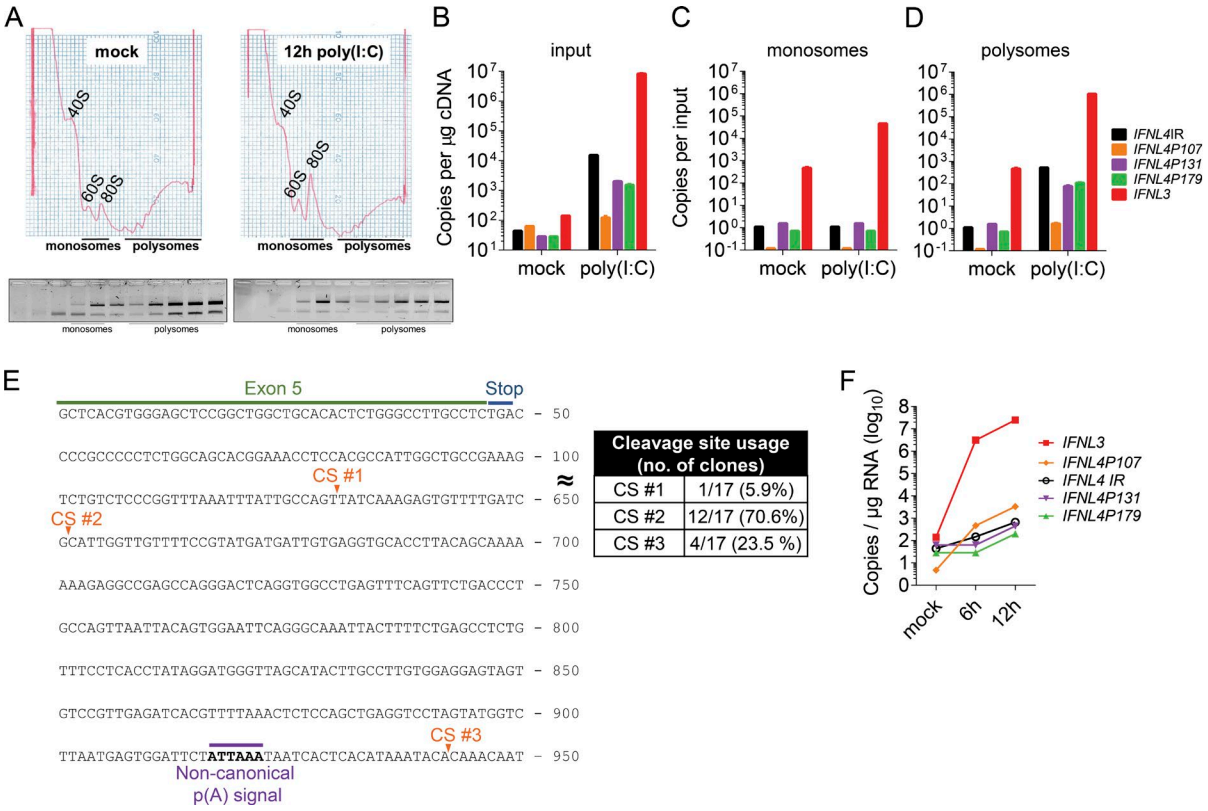

Figure 5. ***IFNL4* mRNA are poorly loaded onto polyribosomes for translation.** (A) Whole-cell extracts from mock- or poly(I:C)-treated HepG2 cells were resolved by density sedimentation in 10–50% sucrose gradients. The UV absorbance trace (254 nm) obtained during fractionation is shown with the positions of the 40S, 60S, 80S, and polyribosomes. The bottom panel shows an agarose gel of polysome fractions to check for 28S and 18S ribosomal RNA in the fractions. (B–D) Copy number expression of *IFNL3* and *IFNL4* isoforms in input (B), monosome (C), and polysome (D) fractions measured by qPCR. (E) Cleavage sites (CS) and frequency of CS usage in the human *IFNL4* 3′ UTR determined by 3′ RACE. (F) Gene expression of *IFNL3* and *IFNL4* isoforms in gorilla fibroblasts upon stimulation with poly(I:C). Representative of two to three independent experiments.

used by *IFNL4* mRNA for termination (Fig. 5 E). More importantly, 70.6% of the analyzed sequences used the second cleavage site (CS#2) followed by CS#3 (23.5%) and CS#1 (5.9%). Intriguingly, the 5′ ends of CS#2 (major cleavage site) and CS#1 (minor cleavage site) do not encode for a canonical or noncanonical polyA signal. Only a small percentage of *IFNL4* mRNA sequences use CS#3, where a weak noncanonical polyA signal (AUUAAA) was detected, suggesting that this is not the major termination site. Previous studies have shown that eukaryotic mRNA does not tolerate changes in these nucleotide motifs and the efficiency of mRNA termination, polyA, and translations are severely hampered (Proudfoot, 2011). Therefore, we propose that the majority of *IFNL4* mRNA that is not efficiently terminated, is rapidly degraded and weakly translated. Overall, basal low-levels of in-frame *IFNL4* mRNA expression and poor translation lead to lack of IFNλ4 protein expression.

Nonfunctional *IFNL4* splice variants arose before the ΔG>TT frame-shift variant in humans

Our studies suggest that IFNλ4 mediates comparable antiviral activity to IFNλ3, but its action is limited through mechanisms including poor endogenous expression, expression of nonfunctional alternative splice variants, isoforms with intron retention, a frame-shift mutation that begets a premature stop codon (ΔG>TT), and the absence of a canonical polyA signal. As nonhuman primates do not carry the ΔG>TT frame-shift mutation and therefore have the potential to express full-length *IFNL4*, it is possible that humans have evolved multiple strategies for limiting the production of IFNλ4 for yet unknown reasons. We hypothesized that if IFNλ4 was detrimental to the host, we would observe such selection in nonhuman primates. Therefore, we stimulated *Gorilla gorilla* fibroblasts with poly(I:C) and found that they also expressed nonfunctional *IFNL4P107* and *IFNL4P131* isoforms, as well as unstable splice variants with intron retention (Fig. 5 F). Like in humans, expression levels of functional *IFNL4P179* were low.

Conclusion

IFNL4 is a member of the type III IFNs that was most recently identified through a genetic association study (Prokunina-Olsson et al., 2013). Genetic studies postulate a cell-autonomous, intracellular role for IFNλ4 in dampening

the antiviral response, but have failed to provide functional support for this hypothesis. Therefore, we performed a comprehensive biochemical and molecular study to investigate the functional role of IFNλ4 during viral infections.

Our IFNλ4 overexpression studies show that the IFNλ4p179 variant can be secreted and has comparable antiviral activities to IFNλ3, confirming previous data (Hamming et al., 2013; Lu et al., 2015a). We extended these observations by producing recombinant full-length IFNλ4p179 protein in *Drosophila* S2 cells, further demonstrating that antiviral activity of IFNλ4 is preserved and its potency against viruses such as HCV and WNV is comparable to that of IFNλ3. We further observed that neither intracellular nor secreted IFNλ4 isoforms interfered with type I or III IFN signaling, as they did not affect induction of ISGs via either type I or type III IFN receptors. These observations are paradoxical to the findings from genetic association studies in HCV patients, where the ΔG allele that codes for full-length *IFNL4P179* associates with a worse clinical outcome (Bibert et al., 2013; Prokunina-Olsson et al., 2013; Aka et al., 2014).

We proceeded to examine whether endogenous IFNλ4 acts similarly during PAMP stimulations or viral infection. By cloning endogenous *IFNL4* isoforms from stimulated hepatocytes, we found additional mRNA splice variants with intron retention in the cDNA, which would not be translated as the introns prevent their export to the cytoplasm. This discovery warranted a comprehensive expression profiling analysis of *IFNL4* isoforms induced in multiple cell lines and primary human hepatocytes containing both variants at rs368234815 (ΔG and TT) during stimulation with PAMP and upon viral infections. Although previous studies documented induction of *IFNL4* (Amanzada et al., 2013), they have used primer/probes that do not differentiate the isoforms and in most cases amplify functional and nonfunctional isoforms indiscriminately. Using qPCR probes specific for each transcript, we were surprised to find that the intron-retaining and *IFNLP107* isoforms were the most abundant among all *IFNL4* isoforms regardless of their rs368234815 genotype. Intron-retaining transcripts are usually targeted for nonsense-mediated decay, and in recent years this process has been recognized as an efficient way to control expression of particular transcripts under different developmental phases or environmental contexts (Hamid and Makeyev, 2014). Therefore, we hypothesize that preferential expression of the intron-retaining isoforms suppresses expression of functional *IFNL4P179*. More intriguingly, *IFNL3* was induced several (two to three) logs-fold higher than any *IFNL4* splice forms. This induction pattern was consistent irrespective of PAMP stimulations or viral infections. We propose two main reasons for inefficient translation of *IFNL4* mRNA. First, multiple isoforms of *IFNL4*, including intron-retaining variants, are induced upon viral infection or stimulation with viral PAMP. Expression of multiple splice variants, especially nonprotein-coding transcripts, may reduce transcriptional resources for expression of the only functionally active *IFNL4P179* isoform. Second, we determined that endogenous *IFNL4* isoforms are not efficiently translated into proteins compared with *IFNL3*, as they are poorly loaded onto polyribosomes upon PAMP stimulation. Notably, *IFNL4* is the only *IFNL* gene that does not encode a strong canonical polyA signal, which recruits proteins that cleave and polyadenylate the primary mRNA. PolyA sequences then lead to the recruitment of several RNA-binding proteins essential for mRNA stability and subsequent translation. Longer polyA tails provide higher mRNA stability and higher translation potential (Proudfoot, 2011). Indeed, we found poor usage of its noncanonical polyA signal. Based on these data, we hypothesize that the *IFNL4* 3′ UTR could be playing additional roles in reducing the expression levels and lowering the translation potential of *IFNL4*.

Altogether, we show that multiple mechanisms combine to minimize IFNλ4 protein expression in the host, including alternative splicing of *IFNL4* for significant production of nonfunctional proteins, preferential expression of unstable intron-retaining mRNA variants, poor loading onto polyribosomes for protein production, and a weak polyA signal that further lowers the stability and translation potential of all *IFNL4* splice forms (Fig. 6). In addition to these regulatory controls, humans have evolved a frame-shift ΔG>TT mutation that further disrupts the coding potential of the *IFNL4* gene. Although nonhuman primates bear only the ancestral ΔG allele, and thus do not have this recent adaptation, we documented favored induction of nonfunctional *IFNL4* isoforms compared with the functional *IFNL4P179* isoform in gorilla fibroblasts, as we observed in human cells.

Our mechanistic evidence shows that humans have sustained adaptations suppressing IFNλ4 activity even when the genotype at rs368234815 allows production of in-frame IFNλ4. Our data suggest that the expression of functional *IFNL4P179* isoform has been selected against in nonhuman primates even before the dinucleotide frame-shift mutation (ΔG>TT) evolved in humans. We propose that splicing and translational control mechanisms to suppress expression of functional IFNλ4 protein appeared before the frame shift mutation that evolved in humans to further silence its expression. Collectively, this study highlights differential activities of the *IFNL* genes during viral infection and the relatively low contribution of *IFNL4* compared with *IFNL3* in physiological immune contexts. The answer to the question of why bioactive *IFNL4* expression is so greatly suppressed, but not *IFNL3*, can only be speculated. Similar to other IFN/cytokine genes, *IFNL4* may have arisen from gene duplication but failed to subfunctionalize or neofunctionalize, leading to high redundancy with *IFNL3*. It is also possible that *IFNL4* may have more complex pathological roles detrimental to the host, which led to its suppression. These are just speculations that can be tested only if the functional *IFNL4* is expressed at physiological levels during infection. We and others have previously found the *IFNL3*

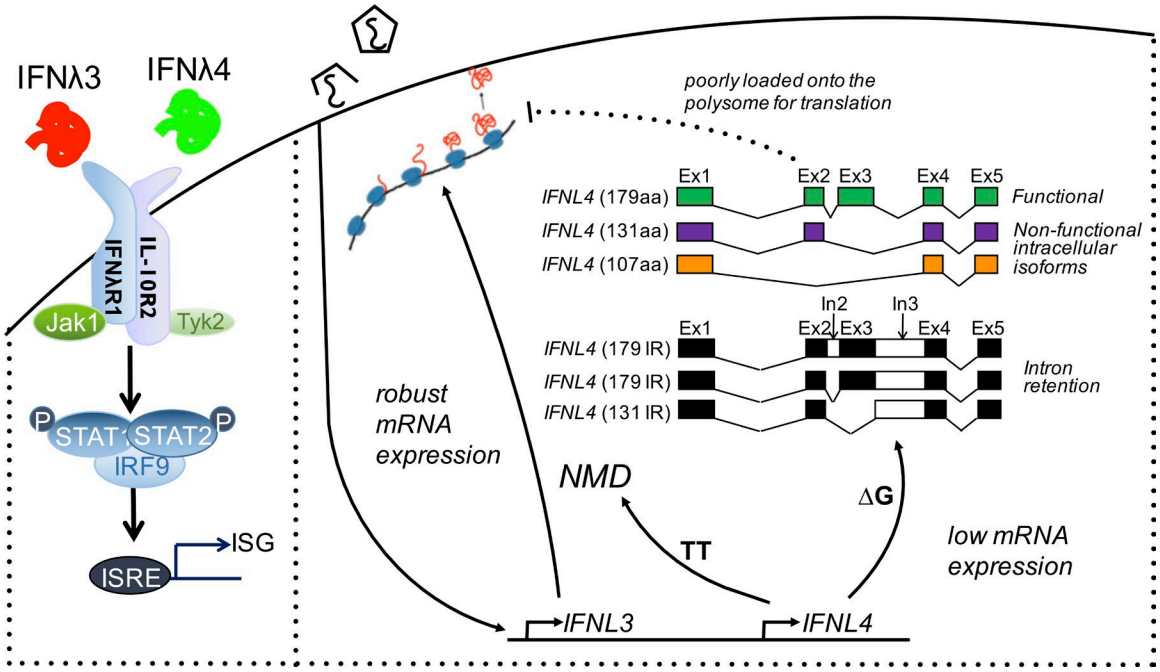

Figure 6. **IFNλ4 expression is suppressed during viral infections.** IFNλ4p179 has similar antiviral properties as IFNλ3, signaling exclusively through the extracellular IFNλR1 and IL-10R2 heterodimer to activate STAT1 and induce ISGs. During viral infections, several mechanisms are in place that suppress the expression of the functional *IFNL4* isoform compared with robust *IFNL3* expression.

variant to have functional effects on antiviral immunity against HCV infection and, unfortunately, high linkage disequilibrium makes it difficult to distinguish the contributing effects of individual polymorphism. It remains to be seen whether the clinical association of *IFNL4* gene expression with poor HCV clearance is simply explained by the tightly linked genetic association of the unfavorable *IFNL4* ΔG genotype with the unfavorable *IFNL3* genotypes and not a direct biological effect of *IFNL4*.

MATERIALS AND METHODS

Cell culture conditions

HepG2, PH5CH8, Huh7, HeLa, HEK293 cells, and *Gorilla gorilla* fibroblasts were cultured in complete DMEM (cDMEM; Sigma-Aldrich) media containing 10% heat-inactivated FBS (Atlanta Biologicals) and 1% penicillin-streptomycin-glutamine (PSG; Mediatech). The cells were incubated at 37°C with 5% CO_2. Primary human hepatocytes (PHH) were purchased from Life Technologies and cultured according to the vendor's instructions. THP-1 cells were grown in complete RPMI 1640 containing 10% FBS, PSG, 10 mM HEPES, 1 mM sodium pyruvate, 1X nonessential amino acids (Mediatech), and 50 µM 2-mecaptoethanol (Sigma-Aldrich). MUTZ-3 cells were grown in MEMα containing nucleosides (Gibco), 20% FBS, and 10% conditioned medium from 5637 renal carcinoma cells. To differentiate myeloid cell lines into dendritic cells, THP-1 and MUTZ-3 cells were seeded at 0.2 × 10^6 cells/ml and cultured for 7 d in the presence of cytokines (for THP-1, 100 ng/ml GM-CSF and 100 ng/ml IL-4 in complete RPMI 1640; for MUTZ-3, 100 ng/ml GM-CSF, 10 ng/ml IL-4, and 2.5 ng/ml TNF in MEMα containing nucleosides, 20% FBS), with half the medium replaced every 3 d.

Generation of *IFNLR1*$^{-/-}$ hepatocytes

IFNLR1 targeting guide RNA (gRNA, 5′-GCTCTCCCA CCCGTAGACGG-3′) was cloned downstream of the U6 promoter in the pRRLU6-empty-gRNA-MND-cas9-t2A-Puro vector using In-Fusion enzyme mix (Takara Bio, Inc.). Hepatocytes were transfected with either cas9-expressing or *IFNLR1* gRNA-cas9–expressing plasmids. For transfection of Huh7 cells, 3 × 10^6 cells were seeded onto a 10-cm dish and 10 µg of plasmid was transfected using the $CaPO_4$ transfection kit (Invitrogen) according to the manufacturer's instructions. After 48 h, cells were preselected by addition of 2 µg/ml puromycin to the media for 2 d. To confirm successful gene targeting in preselected cells, genomic DNA was extracted from wt/cas9 control and *IFNLR1*$^{-/-}$ cells (NucleoSpin Tissue; Takara Bio, Inc.) and subjected to T7 endonuclease I assay. Preselected cells were then single-cell sub-cloned and analyzed for *IFNLR1*$^{-/-}$ knockout efficiency by checking for downstream activation of STAT1 and *MX1* induction upon stimulation with IFNλ3.

Stimulations

IFNβ was purchased from PBL and used at 100 IU/ml. IFNλ3 was purchased from R&D Systems and used at 100 ng/ml. Neutralizing IL-10R2 antibody (MAB874; R&D Systems)

was preincubated with cells at 2–6 μg/ml for 1 h before cytokine stimulation. Poly(I:C) (InvivoGen) was used at 1 μg/ml. The RIG-I ligand HCV 5′ppp RNA (HCV PAMP) was transcribed in vitro and used at 1 μg/ml. Both were transfected into cell lines using XtremeGene HP (Roche) or Mirus TransIT-X2 reagent (Mirus). Primary human hepatocytes were stimulated by adding 1 μg/ml poly(I:C) directly to the culture media.

Cloning and sequencing of *IFNL4* isoforms

We amplified *IFNL4* from HepG2 cells stimulated with poly(I:C) for 12 h and the mRNA was amplified with IFNL4-cDNA fwd and IFNL4-cDNA rev primers (Table S2). The amplified products were cloned into a pCR2.1 TA-cloning vector (Invitrogen) and the inserts were sequenced. *IFNL4P107*, *IFNL4P131*, and *IFNL4P179* were cloned into a C-terminal HA vector [pCMV-HA(c) pHOM-Mem1]. The three isoforms were amplified using the primers IFNL4-FL-HA-fwd and IFNL4-FL-HA-rev (Table S2) and cloned into the vector using EcoRI and SpeI restriction sites. To identify 3′ UTR lengths and sequences of endogenous *IFNL4*, 3′ RACE was performed based on the manufacturer's instruction (Invitrogen). IFNL4-RACE-nest1 and IFNL4-RACE-nest2 forward primers (Table S2) were used for 3′ RACE to amplify the 3′ UTR of *IFNL4*. The 3′ RACE products were cloned into a pCR2.1 TA-cloning vector and sequenced as above.

RNA isolation, reverse transcription, and quantification of gene expression

Total RNA was isolated using the NucleoSpin RNA kit (Macherey-Nagel) according to the manufacturer's protocol. cDNA was synthesized from 1 μg total RNA using the QuantiTect RT kit (QIAGEN) according to the manufacturer's instructions. qPCR was performed using the ViiA7 qPCR system with *Taq*Man reagents (Life Technologies) using custom-made isoform-specific *IFNL4 Taq*Man probes (Table S2; IDT), *IFNL3*, *IFNB*, *ACTB, HPRT*, and ISGs *MX1*, *OAS1*, and *ISG15* (Life Technologies). Gene expression levels were normalized to either *ACTB* or *HPRT*.

Immunoblot analysis

30 μg of cell lysates, 10 μl supernatant, or 1 ml TCA precipitated supernatant from cell culture were subjected to SDS-PAGE and transferred to PVDF membranes (Thermo Fisher Scientific). The membranes were then probed in 5% BSA in TBST (Tris-Buffered Saline and Tween-20) or 5% nonfat milk in TBST for IFNλ4 (4G1; Millipore), phospho-STAT1 (Y701; 58D6; Cell Signaling Technology), STAT1 (42H3, Cell Signaling Technology), HA (6E2; Cell Signaling Technology) or β-actin (13E5; Cell Signaling Technology).

IFN bioactivity reporter assay

An IFN-stimulated response element (ISRE)–luciferase reporter construct along with eGFP control and overexpression constructs for IFNλ3 or IFNλ4 isoforms were cotransfected using XtremeGene HP (Roche) into Huh7 cells plated in a 96-well plate. 24 h after transfection, the cells were lysed with 1x Passive Lysis Buffer (Promega) and luciferase and eGFP values were measured using a multi-mode microplate reader (Synergy HT; BioTek).

Culture conditions of S2 cells

Drosophila Schneider 2 cells (S2) were grown in complete Schneider's *Drosophila* Medium (Invitrogen), 10% heat-inactivated FBS, penicillin-streptomycin (Gibco), and 20 μg/ml gentamycin (Amresco).

Production of recombinant IFNλ4 protein

We expressed IFNλ4 in a *Drosophila* S2 cell expression system (Invitrogen). The cells were stably cotransfected with plasmids encoding *IFNL4*-Histag and a blasticidin resistance gene in a ratio of 19:1 using calcium phosphate (Invitrogen). Cells were then passed into ExpressFive serum-free medium (Invitrogen) containing 25 μg/ml blasticidin and scaled up under constant selection to 1 liter suspension cultures at 125 rpm in spinner flasks. At a density of 5.0×10^6 cells/ml, cells were induced by 0.8 mM $CuSO_4$ to produce IFNλ4 for 8 d. Recombinant IFNλ4 protein was isolated from the supernatant by affinity chromatography, eluted in an imidazole gradient on a Ni^{2+}-IDA-based His60 resin (Takara Bio Inc.). The eluate was analyzed by a Coomassie gel to identify enriched fractions, which were subsequently concentrated by ultracentrifugation columns and desalted in PBS using PD-10 columns (GE Healthcare). To remove nonspecifically bound proteins, we performed size exclusion chromatography using an ÄKTA 9 high pressure liquid chromatography system with a Superdex 200 analytical column (GE Healthcare). Finally, we added 0.1% BSA as a carrier protein and froze single-use aliquots in 20% glycerol.

Cell death assays

PH5CH8 cells were treated with either IFNλ4 (100 ng/ml), IFNλ3 (100 ng/ml), or ActD (10 μg/ml; Thermo Fisher Scientific). Cell death and confluence were assessed over time using an IncuCyte (Essen Bioscience) imaging system for 70 h with 100 nM Sytox Green (Thermo Fisher Scientific), which is a cell-impermeable DNA-binding fluorescent dye that stains only dead cells.

Genotyping assays

Genotyping assays were performed using TaqMan primers and probes as previously described (Prokunina-Olsson et al., 2013; Table S2).

Virus infections

HCV-*Renilla* infections were performed as previously described (Liu et al., 2011). In brief, Huh7 cells (1.5×10^5 cells/ml) were plated on 96-well plates in cDMEM and incubated overnight at 37°C to ensure 60–70% confluency. We infected the cells with HCV-*Renilla* (multiplicity of infection, 0.3) diluted in serum-free DMEM in a total volume of 35 μl for 4 h.

The media was replaced with 100 µl cDMEM, and the cell lysate was harvested for luciferase assay 48 h after infection. WNV isolate TX 2002-HC (WNV-TX) was described previously (Keller et al., 2006). Dengue virus type 2 (DV2) stocks were generated from seed stocks provided by A. Hirsch and J.A. Nelson (Oregon Health and Sciences University, Portland, OR). Virus stocks were titered with a standard plaque assay on Vero cells. Huh7 cells were infected at multiplicity of infection of 1–2 with either WNV-TX or DV2, 25 HAU/ml SeV Cantell strain (Charles River) diluted in serum-free DMEM, or mock infected. The virus inoculum was removed 2 h after infection and replaced with cDMEM supplemented with 10% FBS. Total RNA was extracted using the NucleoSpin RNA kit, treated with DNase I (Ambion) and evaluated by real-time qPCR for relative gene expression and intracellular viral RNA levels using SYBR Green (Applied Biosystems). Real-time qPCR methods for quantifying intracellular WNV viral RNA is described previously (Suthar et al., 2010).

Polysome analyses

10×10^6 HepG2 (*IFNL4* ΔG/TT) cells were stimulated with poly(I:C) for 6 h. Cells were then treated with 100 µg/ml of cycloheximide (MP Biomedicals) for 5 min, then washed twice with ice-cold PBS and harvested. The cell pellet was resuspended in polysome lysis buffer and cells were left to lyse on ice for 20 min, then centrifuged at 8,000 *g* for 10 min at 4°C. Supernatants were layered >10–50% sucrose gradient and centrifuged at 36,000 rpm for 2 h 30 min at 4°C. Gradients were fractionated while continuously monitoring absorbance at 254 nm.

Statistical analyses

Statistics were performed using one-way ANOVA in GraphPad Prism 6.0. For Fig. 1 L, multiple comparisons were made against EV-transfected cells; for Fig. 3 (A and B), multiple comparisons were made against mock-treated cells.

Online supplemental material

Fig. S1 shows titration of IL-10R2 antibody. Fig. S2 shows generation and characterization of *IFNLR1*$^{-/-}$ hepatocytes. Fig. S3 shows sequence alignment of intron-retaining *IFNL4* isoforms identified from a cDNA library from HepG2 cells treated with poly(I:C). Fig. S4 shows alignment of 3' UTR sequences of human *IFNL1*, *IFNL2*, and *IFNL3* genes. Video 1 shows that IFNλ4 treatment does not cause cell death. Table S1 lists 37 ISGs and 3 endogenous controls included in the TaqMan qPCR array. Table S2 lists sequences of primers and probes used in the study.

ACKNOWLEDGMENTS

We thank Marion Pepper (U.W. Immunology) and Joshua J. Woodward (U.W. Microbiology) for advice, technical expertise and facilities to produce recombinant protein using *Drosophila* S2 cell expression system, Jazmine P. Hallinan, Rachel Werther and Abigail R. Dietrich (Fred Hutchinson Cancer Research Center, Seattle WA) for technical assistance with size exclusion. Harmit Malik and Matthew Daugherty (Fred Hutchinson Cancer Research Center) for sharing reagents. We thank Snehal Ozarkar, Stephanie Varela, Bryan Chou and Jennifer Look for experimental support, Adelle McFarland, and Emily Hemann for critical reading of the manuscript, and members of the Savan and Gale laboratories for helpful discussions.

This project was funded partly by National Institutes of Health grants AI108765 (R. Savan), AI060389, AI40035 (M. Gale), and CA176130 (C.H. Hagedorn). C. Lim was funded by the National Science Scholarship provided by the Agency for Science, Technology, and Research (A*STAR), Singapore.

The authors declare no competing financial interests.

Author contributions: R. Savan directed the study. R. Savan, M. Hong, J. Schwerk, C. Lim, A. Kell, A. Jarret, J. Pangallo, Y-M. Loo, and S. Liu performed experiments, analyzed the data, and wrote the manuscript. M. Gale and C.H. Hagedorn provided intellectual input.

Submitted: 28 March 2016
Revised: 10 June 2016
Accepted: 4 October 2016

REFERENCES

Aka, P.V., M.H. Kuniholm, R.M. Pfeiffer, A.S. Wang, W. Tang, S. Chen, J. Astemborski, M. Plankey, M.C. Villacres, M.G. Peters, et al. 2014. Association of the IFNL4-ΔG allele with impaired spontaneous clearance of hepatitis C virus. *J. Infect. Dis.* 209:350–354. http://dx.doi.org/10.1093/infdis/jit433

Amanzada, A., W. Kopp, U. Spengler, G. Ramadori, and S. Mihm. 2013. Interferon-λ4 (IFNL4) transcript expression in human liver tissue samples. *PLoS One.* 8:e84026. http://dx.doi.org/10.1371/journal.pone.0084026

Bibert, S., T. Roger, T. Calandra, M. Bochud, A. Cerny, N. Semmo, F.H.T. Duong, T. Gerlach, R. Malinverni, D. Moradpour, et al. Swiss Hepatitis C Cohort Study. 2013. IL28B expression depends on a novel TT/-G polymorphism which improves HCV clearance prediction. *J. Exp. Med.* 210:1109–1116. http://dx.doi.org/10.1084/jem.20130012

Booth, D., and J. George. 2013. Loss of function of the new interferon IFN-λ4 may confer protection from hepatitis C. *Nat. Genet.* 45:119–120. http://dx.doi.org/10.1038/ng.2537

Coccia, E.M., M. Severa, E. Giacomini, D. Monneron, M.E. Remoli, I. Julkunen, M. Cella, R. Lande, and G. Uzé. 2004. Viral infection and Toll-like receptor agonists induce a differential expression of type I and lambda interferons in human plasmacytoid and monocyte-derived dendritic cells. *Eur. J. Immunol.* 34:796–805. http://dx.doi.org/10.1002/eji.200324610

Contoli, M., S.D. Message, V. Laza-Stanca, M.R. Edwards, P.A. Wark, N.W. Bartlett, T. Kebadze, P. Mallia, L.A. Stanciu, H.L. Parker, et al. 2006. Role of deficient type III interferon-lambda production in asthma exacerbations. *Nat. Med.* 12:1023–1026. http://dx.doi.org/10.1038/nm1462

Crotta, S., S. Davidson, T. Mahlakoiv, C.J. Desmet, M.R. Buckwalter, M.L. Albert, P. Staeheli, and A. Wack. 2013. Type I and type III interferons drive redundant amplification loops to induce a transcriptional signature in influenza-infected airway epithelia. *PLoS Pathog.* 9:e1003773. http://dx.doi.org/10.1371/journal.ppat.1003773

Dellgren, C., H.H. Gad, O.J. Hamming, J. Melchjorsen, and R. Hartmann. 2009. Human interferon-lambda3 is a potent member of the type III interferon family. *Genes Immun.* 10:125–131. http://dx.doi.org/10.1038/gene.2008.87

Ge, D., J. Fellay, A.J. Thompson, J.S. Simon, K.V. Shianna, T.J. Urban, E.L. Heinzen, P. Qiu, A.H. Bertelsen, A.J. Muir, et al. 2009. Genetic variation in IL28B predicts hepatitis C treatment-induced viral clearance. *Nature.* 461:399–401. http://dx.doi.org/10.1038/nature08309

Hamid, F.M., and E.V. Makeyev. 2014. Emerging functions of alternative splicing coupled with nonsense-mediated decay. *Biochem. Soc. Trans.* 42:1168–1173. http://dx.doi.org/10.1042/BST20140066

Hamming, O.J., E. Terczyńska-Dyla, G. Vieyres, R. Dijkman, S.E. Jørgensen, H. Akhtar, P. Siupka, T. Pietschmann, V. Thiel, and R. Hartmann. 2013. Interferon lambda 4 signals via the IFNλ receptor to regulate antiviral activity against HCV and coronaviruses. *EMBO J.* 32:3055–3065. http://dx.doi.org/10.1038/emboj.2013.232

Jewell, N.A., T. Cline, S.E. Mertz, S.V. Smirnov, E. Flaño, C. Schindler, J.L. Grieves, R.K. Durbin, S.V. Kotenko, and J.E. Durbin. 2010. Lambda interferon is the predominant interferon induced by influenza A virus infection in vivo. *J. Virol.* 84:11515–11522. http://dx.doi.org/10.1128/JVI.01703-09

Keller, B.C., B.L. Fredericksen, M.A. Samuel, R.E. Mock, P.W. Mason, M.S. Diamond, and M. Gale Jr. 2006. Resistance to alpha/beta interferon is a determinant of West Nile virus replication fitness and virulence. *J. Virol.* 80:9424–9434. http://dx.doi.org/10.1128/JVI.00768-06

Kotenko, S.V. 2011. IFN-λs. *Curr. Opin. Immunol.* 23:583–590. http://dx.doi.org/10.1016/j.coi.2011.07.007

Kotenko, S.V., G. Gallagher, V.V. Baurin, A. Lewis-Antes, M. Shen, N.K. Shah, J.A. Langer, F. Sheikh, H. Dickensheets, and R.P. Donnelly. 2003. IFN-lambdas mediate antiviral protection through a distinct class II cytokine receptor complex. *Nat. Immunol.* 4:69–77. http://dx.doi.org/10.1038/ni875

Liu, S., C.A. Nelson, L. Xiao, L. Lu, P.P. Seth, D.R. Davis, and C.H. Hagedorn. 2011. Measuring antiviral activity of benzimidazole molecules that alter IRES RNA structure with an infectious hepatitis C virus chimera expressing *Renilla luciferase*. *Antiviral Res.* 89:54–63. http://dx.doi.org/10.1016/j.antiviral.2010.11.004

Lu, Y.F., D.B. Goldstein, T.J. Urban, and S.S. Bradrick. 2015a. Interferon-λ4 is a cell-autonomous type III interferon associated with pre-treatment hepatitis C virus burden. *Virology.* 476:334–340. http://dx.doi.org/10.1016/j.virol.2014.12.020

Lu, Y.F., D.M. Mauger, D.B. Goldstein, T.J. Urban, K.M. Weeks, and S.S. Bradrick. 2015b. IFNL3 mRNA structure is remodeled by a functional non-coding polymorphism associated with hepatitis C virus clearance. *Sci. Rep.* 5:16037. http://dx.doi.org/10.1038/srep16037

Mahlakõiv, T., P. Hernandez, K. Gronke, A. Diefenbach, and P. Staeheli. 2015. Leukocyte-derived IFN-α/β and epithelial IFN-λ constitute a compartmentalized mucosal defense system that restricts enteric virus infections. *PLoS Pathog.* 11:e1004782. http://dx.doi.org/10.1371/journal.ppat.1004782

McBride, D. 2013. Genetic variant links hepatitis C virus clearance and treatment response. *ONS Connect.* 28:50.

McFarland, A.P., S.M. Horner, A. Jarret, R.C. Joslyn, E. Bindewald, B.A. Shapiro, D.A. Delker, C.H. Hagedorn, M. Carrington, M. Gale Jr., and R. Savan. 2014. The favorable IFNL3 genotype escapes mRNA decay mediated by AU-rich elements and hepatitis C virus-induced microRNAs. *Nat. Immunol.* 15:72–79. http://dx.doi.org/10.1038/ni.2758

Meissner, E.G., D. Bon, L. Prokunina-Olsson, W. Tang, H. Masur, T.R. O'Brien, E. Herrmann, S. Kottilil, and A. Osinusi. 2014. IFNL4-ΔG genotype is associated with slower viral clearance in hepatitis C, genotype-1 patients treated with sofosbuvir and ribavirin. *J. Infect. Dis.* 209:1700–1704. http://dx.doi.org/10.1093/infdis/jit827

Mordstein, M., G. Kochs, L. Dumoutier, J.C. Renauld, S.R. Paludan, K. Klucher, and P. Staeheli. 2008. Interferon-lambda contributes to innate immunity of mice against influenza A virus but not against hepatotropic viruses. *PLoS Pathog.* 4:e1000151. http://dx.doi.org/10.1371/journal.ppat.1000151

Mordstein, M., E. Neugebauer, V. Ditt, B. Jessen, T. Rieger, V. Falcone, F. Sorgeloos, S. Ehl, D. Mayer, G. Kochs, et al. 2010. Lambda interferon renders epithelial cells of the respiratory and gastrointestinal tracts resistant to viral infections. *J. Virol.* 84:5670–5677. http://dx.doi.org/10.1128/JVI.00272-10

Nice, T.J., M.T. Baldridge, B.T. McCune, J.M. Norman, H.M. Lazear, M. Artyomov, M.S. Diamond, and H.W. Virgin. 2015. Interferon-λ cures persistent murine norovirus infection in the absence of adaptive immunity. *Science.* 347:269–273. http://dx.doi.org/10.1126/science.1258100

O'Brien, T.R., R.M. Pfeiffer, A. Paquin, K.A. Lang Kuhs, S. Chen, H.L. Bonkovsky, B.R. Edlin, C.D. Howell, G.D. Kirk, M.H. Kuniholm, et al. 2015. Comparison of functional variants in IFNL4 and IFNL3 for association with HCV clearance. *J. Hepatol.* 63:1103–1110. http://dx.doi.org/10.1016/j.jhep.2015.06.035

Onabajo, O.O., P. Porter-Gill, A. Paquin, N. Rao, L. Liu, W. Tang, N. Brand, and L. Prokunina-Olsson. 2015. Expression of interferon lambda 4 is associated with reduced proliferation and increased cell death in human hepatic cells. *J. Interferon Cytokine Res.* 35:888–900. http://dx.doi.org/10.1089/jir.2014.0161

Peiffer, K.H., L. Sommer, S. Susser, J. Vermehren, E. Herrmann, M. Doring, J. Dietz, D. Perner, C. Berkowski, S. Zeuzem, and C. Sarrazin. 2016. IFN lambda 4 genotypes and resistance-associated variants in HCV genotype 1 and 3 infected patients. *Hepatology.* 63:63–73. http://dx.doi.org/10.1002/hep.28255

Pott, J., T. Mahlakõiv, M. Mordstein, C.U. Duerr, T. Michiels, S. Stockinger, P. Staeheli, and M.W. Hornef. 2011. IFN-lambda determines the intestinal epithelial antiviral host defense. *Proc. Natl. Acad. Sci. USA.* 108:7944–7949. http://dx.doi.org/10.1073/pnas.1100552108

Prokunina-Olsson, L., B. Muchmore, W. Tang, R.M. Pfeiffer, H. Park, H. Dickensheets, D. Hergott, P. Porter-Gill, A. Mumy, I. Kohaar, et al. 2013. A variant upstream of IFNL3 (IL28B) creating a new interferon gene IFNL4 is associated with impaired clearance of hepatitis C virus. *Nat. Genet.* 45:164–171. http://dx.doi.org/10.1038/ng.2521

Proudfoot, N.J. 2011. Ending the message: poly(A) signals then and now. *Genes Dev.* 25:1770–1782. http://dx.doi.org/10.1101/gad.17268411

Rauch, A., Z. Kutalik, P. Descombes, T. Cai, J. Di Iulio, T. Mueller, M. Bochud, M. Battegay, E. Bernasconi, J. Borovicka, et al. 2010. Genetic variation in IL28B is associated with chronic hepatitis C and treatment failure: a genome-wide association study. *Gastroenterology.* 138:1338–1345: 1345.e1–1345.e7. http://dx.doi.org/10.1053/j.gastro.2009.12.056

Ray, K. 2013. Hepatitis: New gene IFNL4 is associated with impaired clearance of HCV. *Nat. Rev. Gastroenterol. Hepatol.* 10:63. http://dx.doi.org/10.1038/nrgastro.2013.7

Sheppard, P., W. Kindsvogel, W. Xu, K. Henderson, S. Schlutsmeyer, T.E. Whitmore, R. Kuestner, U. Garrigues, C. Birks, J. Roraback, et al. 2003. IL-28, IL-29 and their class II cytokine receptor IL-28R. *Nat. Immunol.* 4:63–68. http://dx.doi.org/10.1038/ni873

Stone, A.E., S. Giugliano, G. Schnell, L. Cheng, K.F. Leahy, L. Golden-Mason, M. Gale Jr., and H.R. Rosen. 2013. Hepatitis C virus pathogen associated molecular pattern (PAMP) triggers production of lambda-interferons by human plasmacytoid dendritic cells. *PLoS Pathog.* 9:e1003316. http://dx.doi.org/10.1371/journal.ppat.1003316

Suppiah, V., M. Moldovan, G. Ahlenstiel, T. Berg, M. Weltman, M.L. Abate, M. Bassendine, U. Spengler, G.J. Dore, E. Powell, et al. 2009. IL28B is associated with response to chronic hepatitis C interferon-alpha and ribavirin therapy. *Nat. Genet.* 41:1100–1104. http://dx.doi.org/10.1038/ng.447

Suthar, M.S., D.Y. Ma, S. Thomas, J.M. Lund, N. Zhang, S. Daffis, A.Y. Rudensky, M.J. Bevan, E.A. Clark, M.K. Kaja, et al. 2010. IPS-1 is essential for the control of West Nile virus infection and immunity. *PLoS Pathog.* 6:e1000757. http://dx.doi.org/10.1371/journal.ppat.1000757

Tanaka, Y., N. Nishida, M. Sugiyama, M. Kurosaki, K. Matsuura, N. Sakamoto, M. Nakagawa, M. Korenaga, K. Hino, S. Hige, et al. 2009. Genome-wide association of IL28B with response to pegylated interferon-alpha and ribavirin therapy for chronic hepatitis C. *Nat. Genet.* 41:1105–1109. http://dx.doi.org/10.1038/ng.449

Terczyńska-Dyla, E., S. Bibert, F.H. Duong, I. Krol, S. Jørgensen, E. Collinet, Z. Kutalik, V. Aubert, A. Cerny, L. Kaiser, et al. Swiss Hepatitis C Cohort Study Group. 2014. Reduced IFNλ4 activity is associated with improved HCV clearance and reduced expression of interferon-stimulated genes. *Nat. Commun.* 5:5699. http://dx.doi.org/10.1038/ncomms6699

Thomas, D.L., C.L. Thio, M.P. Martin, Y. Qi, D. Ge, C. O'Huigin, J. Kidd, K. Kidd, S.I. Khakoo, G. Alexander, et al. 2009. Genetic variation in IL28B and spontaneous clearance of hepatitis C virus. *Nature.* 461:798–801. http://dx.doi.org/10.1038/nature08463